THE ASTROPHYSICAL JOURNAL, 340:729–738, 1989 May 15

AN INFRARED STUDY OF STARBURSTS IN THE INTERACTING GALAXY PAIR ARP 299 (NGC 3690+IC 694)

TAKAO NAKAGAWA,[1,2,3] TETSUYA NAGATA,[3,4] T. R. GEBALLE,[5] HARUYUKI OKUDA,[1,3] HIROSHI SHIBAI,[1] AND HIDEO MATSUHARA[1,4]

Received 1988 July 8; accepted 1988 October 24

ABSTRACT

Extensive infrared observations have been obtained of the three active regions in Arp 299. Multiaperture *JHK* photometry reveals that the colors of the three regions are totally different from each other, and that there are very red nuclei smaller than 4″ in two of them. Multiaperture spectroscopy of the Brγ and the shock-excited H_2 lines shows that both the atomic and molecular lines are spatially extended, indicating that Arp 299 is undergoing an active episode of star formation not only in its nuclei but also well outside of them.

Although there is some evidence that suggests the presence of a compact, active galactic nucleus, a simple starburst model can explain the bolometric luminosities, production rates of ionizing photons, and H_2 line luminosities of each active region in Arp 299. However, each starburst cannot last longer than 10^8 yr.

Subject headings: galaxies: individual (NGC 3690, IC 694) — galaxies: interactions — galaxies: nuclei — galaxies: photometry — infrared: spectra — stars: formation

I. INTRODUCTION

One of the great discoveries of the *Infrared Astronomical Satellite* (*IRAS*) survey is that a set of highly luminous, infrared-bright galaxies is a major constituent of the overall population of galaxies (Soifer *et al.* 1986). Both compact nuclear sources and bursts of star formation are thought to be responsible for these extreme luminosities. In this paper, we term galaxies which possess either of these features "active galaxies."

It has also been shown that a large fraction of the *IRAS* bright galaxy sample consists of interacting systems (Sanders *et al.* 1988). Galactic interactions have been thought to play an important role in triggering starbursts (see, e.g., Larson and Tinsley 1978). Moreover, Sanders *et al.* (1988) proposed that even quasars originate through the merging of gas-rich galaxies. Therefore, detailed observations of interacting systems are very important not only for the study of infrared luminous galaxies but also for the understanding of all types of active galaxies.

The interacting system Arp 299 (Mrk 171) is composed of two galaxies (Arp 1966), which are named NGC 3690 and IC 694. This system is very luminous in the far-infrared ($L_{FIR} = 5.2 \times 10^{11}\ L_\odot$; Soifer *et al.* 1987), and its proximity of 42 Mpc ($cz = 3159$ km s^{-1}; Sanders and Mirabel 1985; $H_0 = 75$ km s^{-1} Mpc^{-1} is assumed throughout this paper) makes it one of the most suitable interacting systems for detailed study.

Gehrz, Sramek, and Weedman (1983, hereafter GSW) found three major active regions in this system from their optical, infrared, and radio observations and named them sources A, B, and C. We will use their nomenclature throughout this paper. Telesco, Decher, and Gatley (1985) mapped Arp 299 at *K* band with 5.″0 and 7.″2 beams, and concluded that sources A and B are the nuclei of IC 694 and NGC 3690, respectively, despite their large offsets from the visual centroids. Source C is not clearly identifiable with either galaxy and is thought to be an active star forming region; it is presumably a direct result of the interaction.

GSW concluded that the activity of source A cannot be explained by their starburst model, because its optical Balmer lines are surprisingly weak in view of its large luminosity at infrared and radio wavelengths. However, Fischer *et al.* (1983) and Beck, Turner, and Ho (1986) detected strong Brackett lines from source A (as well as from source B), and showed that the line emission is not localized to one emission region but spatially extended. Their results imply that UV photons in source A are produced not by a nonthermal nucleus but by a large number of young massive stars, and thus that a starburst is occurring there.

In order to reveal their types of activity and relative contributions, we have made near-infrared multiaperture photometric and spectroscopic observations of the three active regions of Arp 299. The photometric work allows qualitative classifications of the activity to be made. The spectroscopy centered on two kinds of lines. One is the Brγ line of atomic hydrogen. Infrared H I lines provide information on the distribution and condition of young massive stars, and, in addition, especially when they are very broad, can indicate the presence of an active nucleus (DePoy, Becklin, and Geballe 1987). The other is a set of H_2 $v = 1 \rightarrow 0$ lines; they can also be associated not only with starbursts but also with the activity in the nucleus (DePoy, Becklin, and Wynn-Williams 1986). Combining our results and those of others, we discuss the nature of three sources quantitatively.

II. OBSERVATIONS

a) Photometry

The near-infrared photometric observations were made on 1987 May 7 using the NASA Infrared Telescope Facility (IRTF) and its standard InSb photometer. Each of the three regions (sources A, B, and C) was observed in three bands (*J*, *H*, and *K*) with four apertures (4″, 6″, 8″, and 10″). The aperture

[1] The Institute of Space and Astronautical Science.
[2] Department of Astronomy, University of Tokyo.
[3] Visiting Astronomer at the NASA Infrared Telescope Facility, which is operated by the University of Hawaii under a contract with the National Aeronautics and Space Administration.
[4] Department of Physics, Kyoto University.
[5] Joint Astronomy Centre, Hilo, Hawaii.

TABLE 1

MULTIAPERTURE PHOTOMETRY

SOURCE	BAND	APERTURE (arcsec) 4	6	8	10
A.....	*J*	13.14[a]	12.73	12.40	12.17
		8.89[b]	13.0	17.5	21.7
	H	12.05	11.67	11.37	11.15
		15.4	21.9	29.0	35.4
	K	11.31	11.03	10.79	10.61
		19.7	25.6	31.8	37.3
B.....	*J*	12.55	12.18	11.88	11.69
		15.3	21.5	28.4	33.7
	H	11.66	11.23	10.97	10.82
		22.0	32.9	41.7	47.8
	K	11.12	10.63	10.36	10.22
		23.4	36.9	47.3	53.6
C.....	*J*	13.74	13.33	12.90	12.62
		5.10	7.45	11.1	14.3
	H	12.97	12.54	12.16	11.87
		6.60	9.83	14.0	18.2
	K	11.86	11.62	11.34	11.12
		11.9	14.8	19.1	23.4

[a] Flux in magnitude.

[b] Flux in mJy. Calibration uncertainties $\leq 3\%$.

diameters correspond to linear diameters of 0.8 kpc, 1.2 kpc, 1.6 kpc, and 2.0 kpc at a distance of 42 Mpc. HD 106965 was used as a reference star (Elias *et al.* 1982). The positions in Arp 299 were acquired by offsetting from nearby SAO stars and peaking up in the 4″ aperture at *K* for sources A and C and at *J* for source B.

The photometric results are summarized in Table 1 and the two-color diagram is shown in Figure 1. The uncertainties in the absolute fluxes are less than 3%. The filled circles in Figure 1 indicate the results of multiaperture photometry, and the open circles show annular colors calculated from the above photometric results.

b) Spectroscopy

Two sets of spectroscopic observations in the *K* band were made in 1987 May.

The first set of observations was made using the IRTF and its 32 element Cooled Grating Array Spectrometer (CGAS). A 2″.7 (0.5 kpc) aperture was used with an instrumental velocity resolution of 280 km s^{-1}. The target lines were H_2 $v = 1 \rightarrow 0$ *S*(1) and H I Brγ ($n = 7 \rightarrow 4$). The three regions in Arp 299 and a reference star SAO 28025 (G5) were observed at a single grating position, which allowed the spectral region 2.13–2.20 μm to be covered.

The Arp 299 spectra were divided by that of the reference star, which was assumed to be a 5000 K blackbody. The divided spectra were then smoothed with a 1-2-1 Hanning function, reducing the effective resolution to 630 km s^{-1}. The final spectra are shown in Figure 2. The solid curves in Figure 2 are least-squares fits containing two Gaussian profiles and a linear continuum. The derived intensities of the lines are given in Table 2. Simple Gaussian profiles with the effective resolution described above fit the observed data very well except for the Brγ line in source A, where the continuum level at wavelengths longer than the Brγ line is not well determined. If the Brγ line in source A is broader than we assumed, the intensity listed in Table 2 is a lower limit.

The second set of observations was made at the United Kingdom Infrared Telescope (UKIRT) using its seven-element Cooled Grating Spectrometer (CGS II). All spectra were sampled every one-third of the resolution. The H_2 $v = 1 \rightarrow 0$ *S*(1) line was observed in the three regions with 1100 km s^{-1} resolution and with a 5″ (1.0 kpc) beam, and again was detected only from source A. BS 4550 (G8) was observed as a reference.

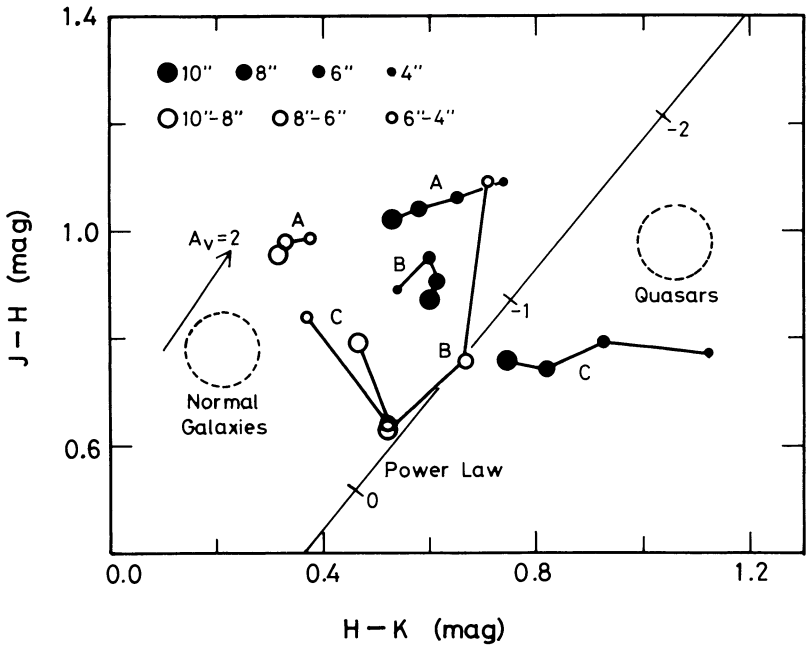

FIG. 1.—The near-infrared color-color diagram of the active regions of Arp 299. Filled circles indicate the results of multiaperture photometry. Open circles show annular colors derived from the above results. The color of normal galaxies is from Glass (1984), and the color of quasars (zero redshift) is from Hyland and Allen (1982). Both are corrected for differences of photometric systems. The arrow of A_V is derived assuming the standard extinction law (Savage and Mathis 1979).

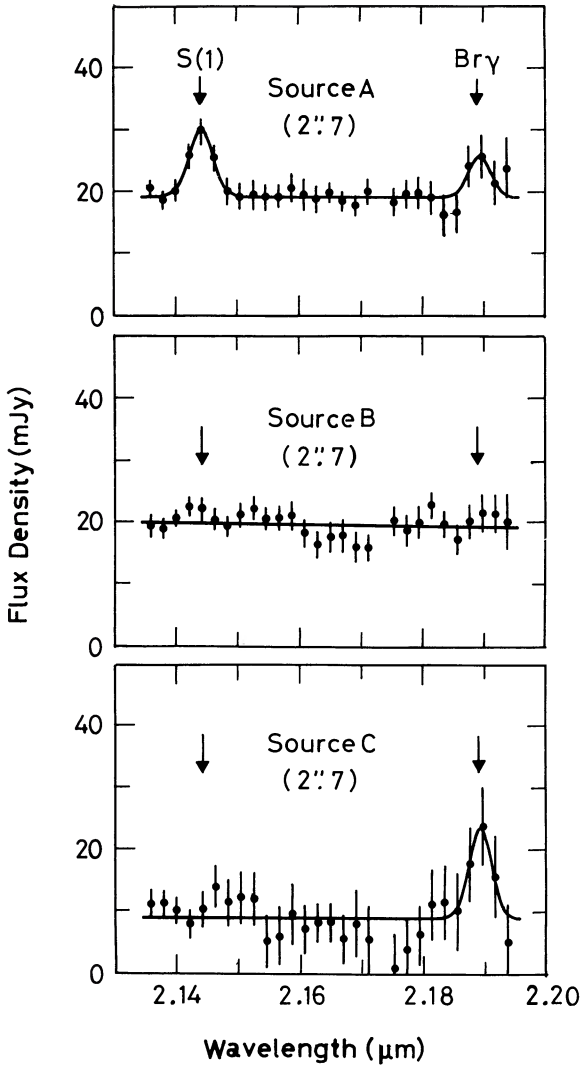

FIG. 2.—Spectra of three active sources in Arp 299 in a 2".7 beam. Solid lines are the least-squares fits containing two Gaussian profiles of effective resolution (see text) and a linear continuum. Two arrows indicate the expected positions of the H_2 $v = 1 \rightarrow 0$ $S(1)$ line and the Brγ line with $cz = 3159$ km s^{-1}.

TABLE 2

OBSERVED LINE INTENSITIES[a]

Line	Aperture	Source A	Source B	Source C
$S(1)$	2".7	3.5 ± 0.7	≤ 1.8	≤ 1.8
Brγ	2.7	1.9 ± 0.7	≤ 1.7	4.1 ± 1.2
$S(1)$	5	4.5 ± 1.2	≤ 3.1	≤ 2.4
$Q(1) + Q(2)$	5	6.1 ± 0.9	...	...
$Q(3)$	5	2.5 ± 0.7	...	...

[a] The unit of line intensities is 10^{-17} W m^{-2}. The flux uncertainties are 1 σ levels and include 15% calibration uncertainties. The upper limits are 2.5 σ statistical uncertainties.

An H_2 $v = 1 \rightarrow 0$ Q-branch spectrum was also obtained for source A. At this wavelength, the resolution was slightly higher (1000 km s^{-1}). BS 4295 (A0) was observed as a reference.

The source spectra were divided by those of the reference stars, which are assumed to be blackbodies. The divided spectra were then smoothed with a 1-2-1 Hanning function, reducing the effective resolution to 1300 km s^{-1} at the $S(1)$ line and to 1200 km s^{-1} at the Q-branch. Final results are shown in Figure 3, together with least-squares fits shown by solid lines, and the derived intensities of the lines are given in Table 2. Although we use three Gaussian profiles [each for $Q(1)$, $Q(2)$, and $Q(3)$] and a linear line (for continuum) to fit the observed data for the Q-branch, we tabulate the derived intensities only for $Q(3)$ and for the sum of $Q(1)$ and $Q(2)$, because the $Q(1)$ and $Q(2)$ lines were not resolved.

The 1 σ error bars shown in Figures 2 and 3 include only statistical fluctuations. We estimate calibration uncertainties to be 15%. The errors of the intensities in Table 2 include both uncertainties.

c) *Atmospheric Absorption*

In order to check the reliability of our spectroscopic results, especially those of Q-branch lines, we have made a theoretical calculation of the atmospheric transmission on Mauna Kea on the basis of the model described by Traub and Stier (1976). We took the basic data from the magnetic tape version of the AFGL molecular absorption data base "HITRAN" (Rothman *et al.* 1987). The column density of the atmospheric H_2O was assumed to be 3.35×10^{21} cm^{-2} or 1 precipitable mm. The

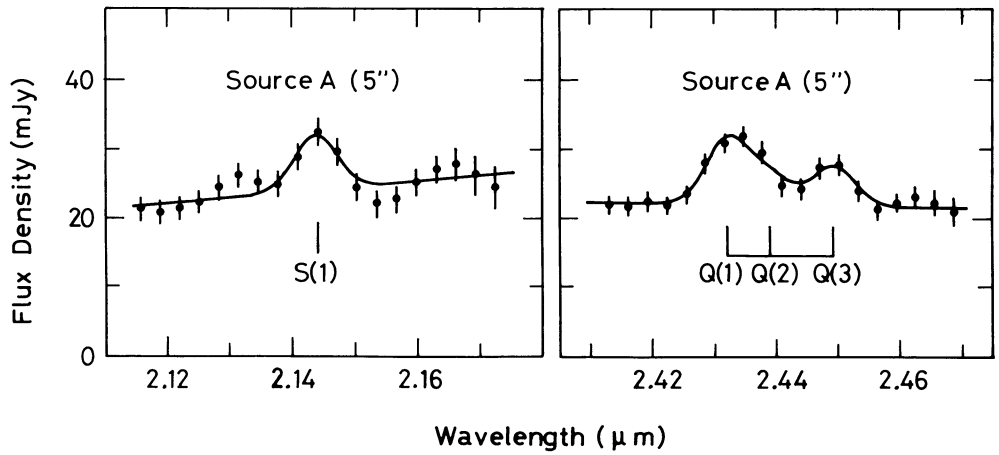

FIG. 3.—Spectra in a 5" beam of the H_2 lines in source A. Solid lines are least-squares fits with a linear continuum and one Gaussian profile [$S(1)$] or three Gaussian profiles (Q-branch). Vertical bars show the expected positions of the H_2 $v = 1 \rightarrow 0$ lines with $cz = 3159$ km s^{-1}.

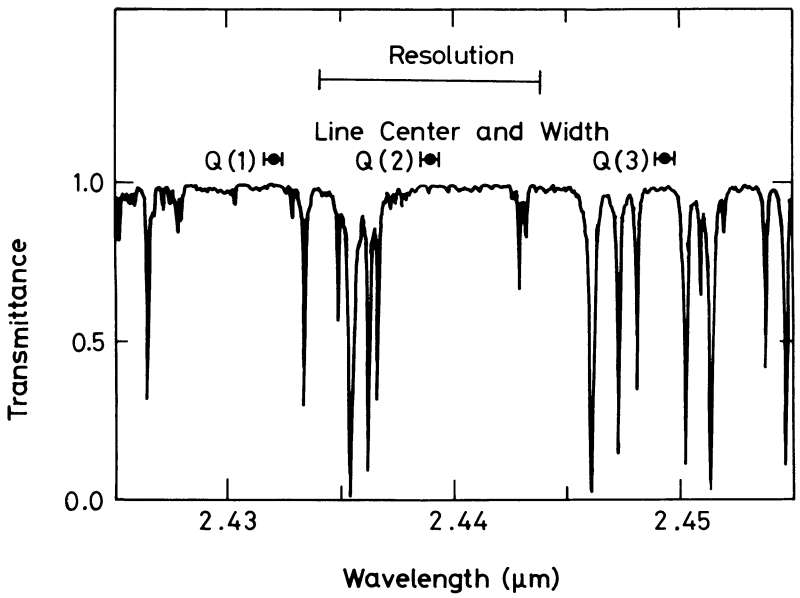

FIG. 4.—Theoretical atmospheric transmission near redshifted Q-branch lines of H_2 on Mauna Kea. The column density of water is assumed to be 1 precipitable mm. The calculation step is 5×10^{-3} cm^{-1}, and the result is smoothed with a Gaussian profile (FWHM = 10 km s^{-1}). Expected line positions (cz = 3159 km s^{-1}), line widths (100 km s^{-1}), and the effective resolution (1200 km s^{-1}) are also shown.

calculation step was 5×10^{-3} cm^{-1}. The result, which was smoothed with a Gaussian profile of 10 km s^{-1} FWHM, is shown in Figure 4. Positions and widths of Q-branch lines, which were estimated on the basis of the redshift (3159 km s^{-1}) and the line width (FWHM = 100 km s^{-1}) of the radio CO observation (Sanders and Mirabel 1985), are also shown in Figure 4, together with the effective resolution (§ II*b*) of our observation.

It is clear from Figure 4 that the atmospheric condition for the $Q(3)$ line is the worst. However, if the width and the position of the line are as expected, most of the $Q(3)$ line does not suffer from the atmospheric absorption. Thus the line intensity is not heavily underestimated. Moreover, because the average atmospheric transmission in the resolution element containing the line is high (~80%), the line strength is not overestimated by more than 20%. Therefore, we conclude that all of the measured line intensities listed in Table 2 are accurate to within the uncertainties given in Table 2, and we use the intensities in the discussions below.

III. RESULTS

a) Color

The colors of the three sources, derived from Table 1, show good agreement with those observed in a 5″ beam by Telesco, Decher, and Gatley (1985); each of the three sources is redder than a normal galaxy (Frogel *et al.* 1978; Glass 1984). However, their positions in the two-color diagram (Figure 1) are quite different from each other.

The colors of source A appear similar to those of Seyfert galaxies (Ward *et al.* 1982; Glass and Moorwood 1985). However, the annular colors of source A (indicated by open circles in Fig. 1), which do not change from 4″ to 10″, can be accounted for by a normal galaxy obscured by $A_v = 2.2$ mag. Therefore, the near-infrared colors of source A can be explained by a mixture of a normal galaxy and another component: a nucleus with power-law spectrum (Glass and Moorwood) or a quasar-like nucleus (Ward *et al.*). It is interesting that the line in Figure 1 connecting the locus of points of the multiaperture photometry for source A is almost parallel to the line which connects normal galaxies and zero redshift quasars (Hyland and Allen 1982). Thus the reddening is almost the same both for the normal galactic component and for the quasar-like nucleus, whose apparent intensity is estimated to be 10 mJy at K. This uniform reddening implies the presence of a considrable amount of dust outside the main body of source A. This dust and associated gas may have been removed from the main body as a result of the interaction.

The locus of points for source C in Figure 1 also indicates the presence of a red nucleus which is smaller than 4″ (0.8 kpc) in diameter. However, the colors cannot be explained by adding a power law spectrum to that of a normal galaxy. The addition of a hot dust component, which makes the $H-K$ color redder while changing the $J-H$ color little (Telesco, Decher, and Gatley 1985; Glass and Moorwood 1985), can improve the fit. The combination of a normal galaxy and a hot dust component with $T = 600$ K and $f_\nu = 8$ mJy at K ($\epsilon \sim \lambda^{-1}$ is assumed) fits the colors very well. The annular colors of source C are different from those of source A and indicate that the hot dust component is extended around source C.

Although we interpret the colors of sources A and C as combinations of two components as described above, Telesco, Decher, and Gatley (1985) interpret the color of source A as a combination of three components (a normal galaxy, H II regions, and reddening), and the color of source C as a combination of four components (the same three components described above and hot dust). However, we believe that our simple combination of two components, normal galaxies and redder nuclei, is preferable because (1) the loci of multiaperture photometry in the two-color diagram are quite linear and (2) the larger annular regions of both sources have bluer colors.

The locus of points for source B in the two-color diagram is rather complicated. It does not show a consistent tendency as the aperture changes. The 6″–4″ annular region is much redder than the 4″ central region around the peak at J and has similar

color to that of source A. We are not sure whether this suggests the existence of a redder component in the annular region or implies that the peak position changes with wavelength. Eales *et al.* (1987) resolved source B into two components which are separated by 2".5 and have totally different colors. It may be this two-component structure that makes it difficult to interpret the color of source B. In any case, it is at least certain that source B is not simply dominated by a bright nucleus.

b) Extinction

In order to evaluate quantitatively the star-forming or other nuclear activity, we have derived extinctions in Arp 299 from our data and others', assuming the same extinction law as in our Galaxy (Savage and Mathis 1979). The results are summarized in Table 3.

The extinction toward H II regions is estimated from the observed ratios of recombination lines. We assume Menzel case B (Osterbrock 1974; Giles 1977) and adopt $T = 10^4$ K and $n_e = 10^4$ cm^{-3}. In Table 3, one can see a large discrepancy between the A_V's derived from different pairs of recombination lines. We adopt the A_V's derived from Brackett lines, because they can penetrate heavily obscured regions and probably provide the best estimates of the extinction.

Although we cannot estimate the extinction toward source C from the ratio of Brackett lines alone, all of the observed ratios of Balmer and Brackett lines show that source C is less obscured than sources A and B (Table 3). This is consistent with the small extinction obtained from the silicate absorption feature for source C (GSW).

Combining the values obtained through these procedures, we adopt $A_V = 13$ mag, 14 mag, and 5.5 mag toward H II regions in sources A, B, and C, respectively.

It should be noted that the relative extinctions to the H II regions in sources A and B are rather puzzling. As described above, the Brγ/Brα ratio (Beck, Turner, and Ho 1986) shows that source B has roughly the same amount of obscuration as source A. However, source B should be much more obscured than source A, because the Brα line is weaker in source B by 17% than in source A (Beck, Turner, and Ho), while the Hα line is at least 2.5 times brighter in source B than in source A (GSW). On the contrary, both the silicate absorption feature and the radio CO emission indicate that source B is much less obscured than source A.

Both this inconsistency in the extinction estimates and the complicated near-infrared colors described in § III*a* suggest that source B consists of multiple components. If so, the extinction derived above for source B may not apply to any of its individual components.

Next, we estimate the extinction toward H_2 line-emitting regions from the observed ratio of the $Q(3)$ and $S(1)$ lines, whose intrinsic ratio is always 0.7. Our 5" aperture observations show this ratio to be 0.5 ± 0.3, which means $A_V < 8.5$ mag. This is a surprisingly low extinction for shocked H_2 and indicates that the H_2 line emission may be occurring in rather diffuse molecular gas (see also § III*c*).

Photometric results indicate a uniform extinction of $A_V = 2.2$ mag toward source A (see § III*a*). Therefore, the A_V toward the H_2 line-emitting regions in source A is probably at least 2.2 mag; we adopt $A_V = 3$ mag toward the H_2 line-emitting regions in source A for later discussions.

It should also be noted that the extinction derived from the radio CO observation (Sanders and Mirabel 1985; Sargent *et al.* 1987) is much larger than the extinction derived from other observations. This is not too surprising because there are large uncertainties in the CO line optical depth, the CO/H_2 ratio, the gas/dust ratio, and the fraction of the CO column density that is in front of sources A, B, and C.

c) Excitation Mechanism for the H_2 Line Emission

The relative intensities of H_2 lines, corrected for the extinction, are listed in Table 4. These values are consistent with shock excitation (e.g., Hollenbach and Shull 1978). However, the most critical lines ($v = 2 \rightarrow 1$ lines) for discriminating between shock and fluorescence have not been measured, and we thus cannot exclude fluorescence. For the present, we assume that most of the observed H_2 is excited by shock waves.

d) Spatial Extent of the Lines

Figure 5 shows the spatial extent of the Brγ and the 1–0 $S(1)$ lines. Filled circles show our results. Filled triangles are from Beck, Turner, and Ho (1986). Filled squares are from Fischer *et al.* (1983), who made spectroscopic observations with two different-sized apertures. One covered all the three regions with a 34" beam, and the other covered only sources B and C with a 21".4 beam. We have estimated the intensities of the lines centered on source A from their observations and indicate those intensities by open squares with crossed error bars; we include the error bars even for the aperture because we cannot define it precisely.

Figure 5 clearly indicates that both line-emitting regions in Arp 299 are spatially extended with dimensions of at least 5 kpc. This result contrasts with that of Joseph *et al.* (1987), who found that the Brγ line is more centrally concentrated than the H_2 $S(1)$ line in NGC 3227 (Seyfert I) and NGC 2798

TABLE 3

EXTINCTION (A_v)

Methods	Beam	Source A (mag)	Source B (mag)	Source C (mag)
Hβ/Hα[a]	3".6 or 5"	...	2.4	1.9
Hα/Brγ[a,b,c]	5	$\geq$4.8	...	2.4
Brγ/Brα[b]	7.2	13	$\geq$14	...
Silicate absorption[a]	5	24	14	5.5
H_2 $S(1)/Q(3)$[c]	5	$\leq$8	...	...
N_{CO}[d]	5	65	$\leq$14	65

NOTE.—We derive all of the above extinction except the last one (N_{CO}), assuming the same extinction law as in our Galaxy (Savage and Mathis 1979). Menzel case B ($T = 10^4$ K, $n_e = 10^4$ cm^{-3}) is assumed for recombination lines.

[a] Gehrz, Sramek, and Weedman 1983.

[b] Beck, Turner, and Ho 1986.

[c] This work.

[d] Sargent *et al.* 1987. However, we adopt half of their values assuming that half of the CO column density is in front of the sources.

TABLE 4

RELATIVE INTENSITIES[a] OF H_2 LINES

LINE (1 → 0)	SOURCE A[b] (1 kpc)	UV[c]	SHOCK[d] (km s^{-1}) 6	10	14
$Q(1) + Q(2)$	1.2 ± 0.5	2.03	1.38	1.04	0.94
$Q(3)$	0.5 ± 0.3	0.70	0.70	0.70	0.70

[a] All intensities are normalized to the $1 \rightarrow 0$ $S(1)$ line.

[b] Observed intensities corrected for the extinction of $A_V = 3$ mag.

[c] Black and Dalgarno 1976.

[d] Hollenbach and Shull 1977.

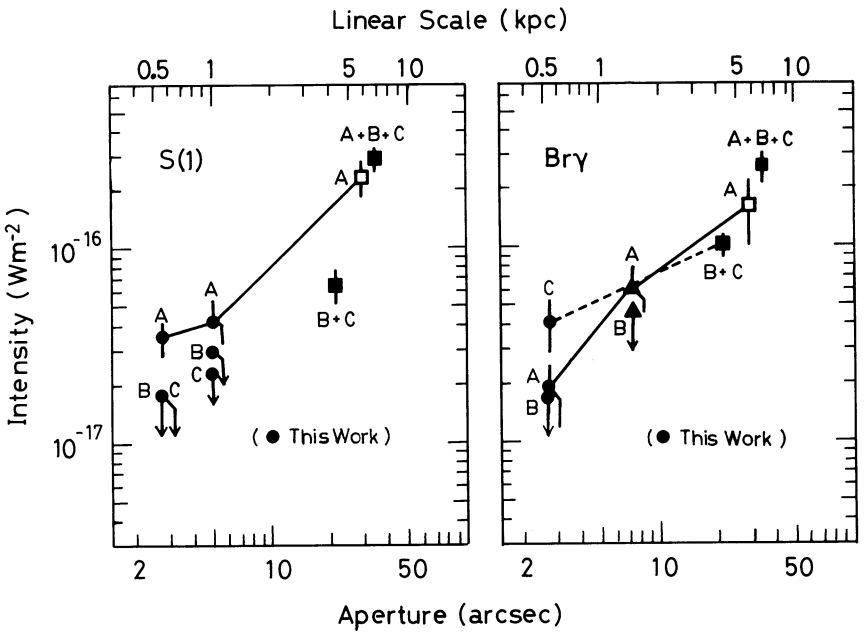

FIG. 5.—Spatial extents of the H_2 $v = 1 \rightarrow 0$ $S(1)$ and Brγ lines. Filled circles are from this work. Filled triangles are from Beck, Turner, and Ho (1986). Filled squares are from Fischer *et al.* (1983). Open squares with crossed error bars are derived from the results of Fischer *et al.* (see text).

(interacting galaxy). On the other hand, observations by Kawara, Nishida, and Gregory (1987) indicate that the two lines are similarly extended in galaxies without active nuclei, while the Brγ line is more centrally concentrated than the H_2 $S(1)$ line in the galaxies with active nuclei.

Arp 299 thus appears to be different in the spatial extent of its atomic and molecular hydrogen lines from galaxies with active nuclei. If its H_2 and H I lines are produced by starbursts, the starbursts are occurring not only in the nuclei but also well outside of them.

Figure 5 also demonstrates that source A dominates the H_2 line emission but not the Brγ line emission. Therefore, source A is different in nature from the other sources. We will discuss this difference in § IV.

e) Scaling the Observational Results

In order to compare the diverse observations with a starburst model, we scale the observed line and continuum fluxes to those in a 5″ (1 kpc at a distance of 42 Mpc) aperture. The results are summarized in Table 5.

TABLE 5

PARAMETERS DERIVED FROM OBSERVATIONS

Source	N_{UV}[a] (10^{54} s^{-1})	$L_{S(1)}$[b] (10^6 $L_\odot$)	L_{FIR}[c] (10^{11} $L_\odot$)	H_2 Mass[d] (10^8 $M_\odot$)
A.....	2.7	3.6	3.1	14
B.....	2.4	<1.0	2.1	<3
C.....	1.6	<0.8		14

NOTE.—Above values are for regions of 5″ (1 kpc) in diameter except for L_{FIR}.

[a] Derived by combining the following observations: this work; Beck, Turner, and Ho 1986; Fischer *et al.* 1983. The extinction described in § III*b* is assumed.

[b] This work. Assumes $A_V = 3$ mag (§ III*b*). The upper limits are 1 σ levels.

[c] Derived by combining the measurement by *IRAS* (Soifer *et al.* 1987) and scanning observations by Joy *et al.* 1989.

[d] Sargent *et al.* 1987.

First, the number of ionizing photons is estimated by combining the observations of the Brackett lines (this work; Beck, Turner, and Ho 1986; Fischer *et al.* 1983). We assume the extinction derived for H II regions in § III*b* and Menzel case B (Osterbrock 1974; Giles 1977), $T_e = 10^4$ K, and $n_e = 10^4$ cm^{-3}. The resultant UV photon rates, N_{UV} (Table 5), are quite large. For comparison, N_{UV} in M82, a typical starburst galaxy, is 3×10^{53} s^{-1} (central 450 pc; Rieke *et al.* 1980).

We should mention that the derived UV photon rates are insensitive to the assumed temperature and density, but could change by a factor of 2 because of the uncertainties in the extinction estimates.

Next, we estimate the bolometric or far-infrared luminosity, combining the total far-infrared luminosity of Arp 299 measured by *IRAS* (5.2×10^{11} $L_\odot$; Soifer *et al.* 1987) and scanning observations by Joy *et al.* (1989). The latter observations at 50 and 100 μm revealed that 60% of the far-infrared luminosity of Arp 299 comes from source A, with the remaining 40% originating in the summed region of sources B and C. The relative contributions from sources B and C are uncertain. We take therefore $L_{bol} = 3.1 \times 10^{11}$ $L_\odot$ for source A and $L_{bol} = 2.1 \times 10^{11}$ $L_\odot$ for the sum of sources B and C. Although the far-infrared radiation could be extended beyond 5″, we believe that the above value for source A is reliable because source A was not resolved in the far-infrared (Joy *et al.* 1989). However the luminosity for the sum of sources B and C is slightly overestimated if the region has low-level extended emission, as is suggested by Joy *et al.*

In order to estimate the intrinsic luminosity of the H_2 emission, we take $A_V = 3$ mag, which was originally derived toward source A, also toward sources B and C. The derived luminosity of $S(1)$ for source A (Table 5) is very large and corresponds to 10^5 Orion-like objects within the 1 kpc diameter region.

IV. STARBURSTS IN ARP 299

a) The Starburst Model

In the previous section, we discussed the observational results and showed that each of the three sources is very active,

but that their natures are diverse. In this section, we search for sources of the activity and explore whether starbursts can explain all the activity or compact, active galactic nuclei are required.

First, we construct a simple starburst model to investigate the natures of the active regions in Arp 299. Our model is based on the model by GSW but includes a time dependence to allow for the evolution of the starbursts.

Our model assumes a power-law initial mass function (IMF):

$$dN = N_0 m^{-\alpha} dm , \quad (1)$$

where dN is the number of stars produced during the starburst per unit time and in a mass interval dm, N_0 is a normalizing constant, and m is the stellar mass.

In our model, the starburst is assumed to have begun T_0 years ago and to have proceeded at a constant rate since then. The lifetime, $\tau(m)$, that a star with mass m is on the main sequence may be longer or shorter than T_0. Therefore, if we define m_0 to be the mass of stars with lifetime of T_0, the number of stars observable at present (dN_p) per mass interval can be written as follows:

$$dN_p = N_0 m^{-\alpha} T_0 \, dm \qquad (m_l \leq m \leq m_0) \quad (2)$$

$$= N_0 m^{-\alpha} \tau(m) dm \qquad (m_0 < m \leq m_u) , \quad (2')$$

where m_1 and m_u are the lower and upper limits of the IMF.

Now, we determine the IMF of our model. First, Augarde and Lequeux (1985) deduced two constraints on the IMF in Arp 299 from their optical and UV spectroscopic observations. One constraint is that the formation of low-mass stars is heavily suppressed, and the other is that the contribution of very luminous stars is not large. On the basis of their conclusions, we assume $m_l = 6\ M_\odot$, allowing m_u to vary between 20 and 45 $M_\odot$. We will discuss the validity of these assumptions in the next subsection. Next, we adopt $\alpha = 2.5 \pm 0.5$ on the basis of the recent determinations of the IMF slope about this mass range (Scalo 1986, 1987).

The normalizing constant N_0 is determined by equating numbers of ionizing photons predicted from our model with those determined from the observations of H I recombination lines (Table 5). The number of ionizing photons (N_{UV}) per unit time produced by the ionizing stars in our model is given by the expression

$$N_{UV} = \int_{m_l}^{m_u} uv(m) dN_p , \quad (3)$$

where $uv(m)$ is the number of ionizing photons produced per unit time by a star with mass m.

The galactic bolometric luminosity L_{bol} produced by the starbursts can be estimated, using the bolometric luminosity $l(m)$ of a star with mass m, as follows:

$$L_{bol} = \int_{m_l}^{m_u} l(m) dN_p . \quad (4)$$

Here we neglect the contribution of pre– and post–main-sequence stars. Because *IRAS* shows that the Arp 299 emits most of its energy in the far-infrared ($L_{FIR}/L_B > 10$; Soifer *et al.* 1987), and L_{FIR} is assumed to be attributed to young massive stars, we can equate L_{bol} with the far-infrared luminosity. If the efficiency of the starburst is fixed, which means the IMF and N_0 are fixed, the bolometric luminosity L_{bol} goes up as the starburst gets older. Therefore, we can constrain the elapsed time T_0 of the starburst by this relation.

We also can estimate supernova rates from our model. Because our model includes only massive stars ($m_l = 6\ M_\odot$), we can assume that every star that has passed its main-sequence lifetime $\tau(m)$ quickly becomes a supernova. Only the massive stars whose lifetimes are shorter than T_0 can contribute to the supernova rate. Consequently, the supernova rate R_{SN} can be written as follows:

$$R_{SN} = \int_{m_0}^{m_u} dN . \quad (5)$$

The total mass of stars (M_{star}) which have been produced during the starburst and are in the form of stars at present is easily estimated from our model as follows:

$$M_{star} = \int_{m_l}^{m_u} m \, dN_p . \quad (6)$$

We take the lifetime $\tau(m)$ of a star from GSW, ionizing photon rates $uv(m)$ from Melnick, Terlevich, and Eggleton (1985), and the bolometric luminosity $l(m)$ from Allen (1976).

b) The Natures of the Starbursts

In this subsection, we compare our model (§ III*a*) with the observations (Table 5). We selected the age T_0 and the upper limit m_u to make the bolometric luminosity L_{bol} and the ionizing photon rates N_{UV} of the model match the observations (Table 5). Because the respective contributions of sources B and C to L_{bol} are uncertain (§ III*e*), we make the comparison only for source A and for the sum of sources B and C.

i) *UV and Far-Infrared Behavior*

The results of our model calculation are displayed in Figure 6; it shows the combinations of the two parameters (m_u and T_0) of the model, which makes the calculated N_{UV} and L_{bol} fit the observations. Because the results in Figure 6 are insensitive to the assumed m_l, we fix the lower limit m_l to be 6 $M_\odot$, while changing the slope α between 2.0 and 3.0. The two lines with hatching in Figure 6 are lifetimes of the lightest and the heaviest stars in the model. Therefore, the L_{bol}/N_{UV} ratio changes with T_0 only between the two lines in Figure 6.

The starbursts in the two regions are significantly different in their ratios of L_{bol} to N_{UV}; source A has a much larger L_{bol}/N_{UV} ratio. There are two factors to increase this ratio.

In order to produce a larger L_{bol} at fixed N_{UV} and T_0, a larger number of less massive stars is required, which means a more rapid rate of star-formation. Therefore, if the age (T_0) of the starburst is fixed, the upper limit m_u is smaller for source A than for the sum of sources B and C as Figure 6 shows.

On the other hand, for a fixed IMF, an older star-forming region produces a larger ratio of L_{bol} to N_{UV}, because the relative number of massive stars, which produce most of N_{UV}, decreases as the starburst gets older. From this point of view, Telesco, Decher, and Gatley (1985) and Augarde and Lequeux (1985) conclude that the starburst in source A is older than is occurring in sources B and C. Figure 6 also suggests the same conclusion.

We cannot distinguish these two factors, because there are two free parameters (m_u and T_0) to make the model fit the observations, and hence we cannot determine each parameter independently. However, if the slope α is fixed, Figure 6 shows that source A clearly requires a smaller upper mass m_u than does the sum of sources B and C while the two regions do not

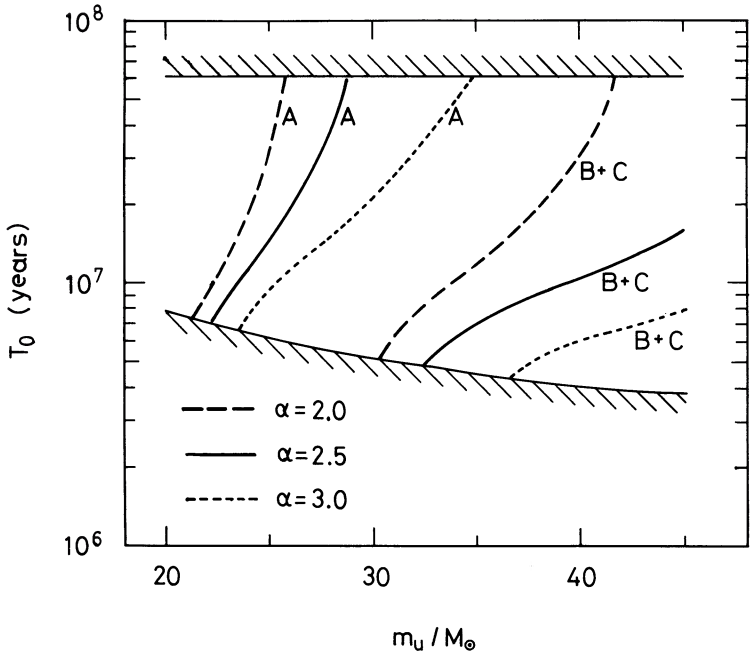

FIG. 6.—Combinations of the two parameters (the upper mass m_u of the IMF and the starburst age T_0) of the starburst model. The parameters are selected to make the calculated N_{UV} and L_{bol} match the observations (Table 5). The lower mass m_l is fixed to be 6 $M_\odot$. The results are shown for three different IMF slopes (α). Two lines with hatching are lifetimes of the lightest and the heaviest stars in the model.

necessarily have different ages. Therefore, we believe that the difference of the upper mass m_u is more essential than that of the ages T_0 to make the properties of the two regions different.

In each case, Figure 6 shows that the observed luminosity (L_{bol}) and ionizing photon rates (N_{UV}) are consistent with our simple starburst model, if the upper mass of the IMF is not too large.

Table 6 shows details of representative models, which are arbitrarily selected from Figure 6.

ii) *Initial Mass Function*

In § IV*a*, we determine m_u and m_l of the IMF according to Augarde and Lequeux (1985). However, they modeled optically observed H II regions which may have a different IMF than do the more obscured regions which we are studying. Therefore we check the validity of the assumed m_u and m_l in this subsection.

First, the upper limit m_u of the IMF can be constrained from the discussions in the previous subsection; we cannot make our model fit the observations of source A if m_u is larger than 35 $M_\odot$ (Fig. 6).

Next, the lower mass m_l is also constrained on the basis of our model. Although neither the luminosities nor the ionizing photon rates are sensitive to the lower mass m_l, the total mass M_{star} increases quickly as m_l decreases. Indeed, if we extend our IMF to 1 $M_\odot$ with $\alpha = 2.5$, the total mass, M_{star}, of stars produced during the starburst in source A exceeds the mass of gas available at present. Moreover, although not decisive, there are several arguments in favor of a deficiency of low mass stars in starburst galaxies (Scalo 1987).

There are many uncertainties in the observations and the assumptions which we use here, and hence the IMF discussed in this section does not provide the only fit to the data. However, on the basis of the discussion in this subsection, we believe that the formations both of very luminous stars and of low-mass stars are suppressed at least in source A.

iii) H_2 *Line Emission*

The two regions, source A and the sum of sources B and C, have significantly different H_2 $S(1)$ luminosities. Forecasting the H_2 radiation from our model is a questionable exercise, because the exact nature of the H_2 line-emitting regions is uncertain. However, we can make a rough estimate in order to check if our starburst model is consistent with the observed $S(1)$ luminosities.

We assume that the H_2 is excited by shock waves in the following two kinds of sources: (1) outflows from pre–main-sequence massive stars and (2) supernova remnants. For the former, we assume that all of the stars ($m \geq 6$ $M_\odot$) in our model undergo episodes like Orion-KL, and maintain $L_{S(1)} = 40$ $L_\odot$ (Fischer *et al.* 1987) for 10^4 yr (Fischer *et al.* 1985; Oliva and Moorwood 1986). For the latter, we adopt the extinction-corrected $S(1)$ luminosity of IC 443 (70 $L_\odot$; Burton *et al.* 1988) and its age of 1.3×10^4 yr (Parkes *et al.* 1977). Then the $S(1)$

TABLE 6

REPRESENTATIVE STARBURST MODELS

Model	m_u ($M_\odot$)	m_l ($M_\odot$)	α	T_0 (10^7 yr)	N_{UV} (10^{54} s^{-1})	L_{bol} (10^{11} $L_\odot$)	$L_{S(1)}$ (10^6 $L_\odot$)	M_{star} (10^8 $M_\odot$)
1 (Source A)	27	6	2.5	2.6	2.7	3.1	1.9	4.6
2 (Sources B + C).....	40	6	2.5	1.1	4.0	2.1	0.9	1.7

luminosity is simply written as follows:

$$(L_{S(1)}/L_{\odot}) = 40 \times 10^4 \int_{m_l}^{m_u} N_0 m^{-\alpha} dm + 70 \times 1.3 \times 10^4 R_{SN} . \quad (7)$$

The $L_{S(1)}$ derived in this way from our model is consistent with the observed upper limit for the sum of sources B and C (model 2 in Table 6) but is smaller than the observed $S(1)$ luminosity for source A (model 1 in Table 6). However, considering the uncertainty in the estimate of the number and intensities of H_2 line-emitting regions, we believe that a significant portion of the H_2 line emission from Arp 299 is excited by the pre–main-sequence massive stars and supernova remnants which have been produced during the starbursts, and the large $L_{S(1)}/L_{Br\gamma}$ ratio in source A is attributable to the rapid rate of the star formation in this region.

However, we cannot exclude other mechanisms, such as ultraviolet pumped fluorescence (e.g., Gatley *et al.* 1987) and large-scale winds from starburst nuclei (Chevalier and Clegg 1985; Heckman, Armus, and Miley 1987; Taniguchi *et al.* 1988).

c) *An Active Nucleus?*

The flat spectrum of the radio compact nucleus (Condon *et al.* 1982; GSW) and the Seyfert-like near-infrared colors (§ III*a*) suggest the presence of an active galactic nucleus in source A. Does a compact, active galactic nucleus really exist in source A?

The two best studied extreme infrared galaxies are Arp 220 and NGC 6240 (see, e.g., Soifer, Houck, and Neugebauer 1987). Their far-infrared luminosities, $L_{FIR} = 4 \times 10^{11}\ L_{\odot}$ for NGC 6240 (DePoy, Becklin, and Wynn-Williams 1986) and $L_{FIR} = 1 \times 10^{12}\ L_{\odot}$ for Arp 220 (Soifer *et al.* 1987), are comparable with that of Arp 299. However, the H I lines are too weak both in Arp 220 and in NGC 6240 for simple starbursts to explain their activity. Furthermore, the evidence for an active nucleus, such as broad H I lines, is strong for them (Soifer *et al.* 1984; Rieke *et al.* 1985; DePoy, Becklin, and Wynn-Williams 1986; DePoy, Becklin, and Geballe 1987).

In contrast to Arp 220 and NGC 6240, no clear evidence of broad H I lines is found in Arp 299 (Fig. 2), and the luminosities and ionizing photon rates are consistent with a simple starburst model (§ IV*b*). Moreover, spatially extended H I and molecular hydrogen lines strongly support the existence of starbursts on a large scale. Recent observations by others also support the starburst model as follows: (1) narrow Hα lines and spatially extended Hα emission observed by Friedman *et al.* (1987) are clearly properties not found in active galactic nuclei, and (2) the temperature gradient observed by Joy *et al.* (1989) in the thermal infrared is against the idea that the active nucleus in source A is a dominant source of the luminosity.

We cannot completely exclude nuclear activity in Arp 299, and it possibly coexists with starbursts in source A, as is suggested by the near-infrared colors and radio observations. However, on the basis of the above discussion, we conclude that the possible nuclear activity does not dominate the luminosity and the line-emission.

d) *Evolution as an Interacting System*

Arp 299 is morphologically different from the sample of ultraluminous galaxies (including Arp 220) of Sanders *et al.* (1988) in the following two ways:

1. The distance between the two nuclei of the interacting galaxies is relatively large (22″). The projected distance is 4.5 kpc.

2. Large-scale tails, which are often characteristic of evolved interacting systems (e.g., Toomre and Toomre 1972), have not been found (Bushouse and Gallagher 1984).

These two facts suggests that Arp 299 is a younger interacting system than other systems which are often called mergers. Our model also suggests that the starbursts, which are results of the galaxy interaction in Arp 299, are very young (Table 6).

Moreover, the starbursts in Arp 299 cannot last for a long time. The M_{star} in Table 6 is not negligible compared to the mass of H_2 (Table 5). If we take the mass consumption rate, $dM/dt = 7 \times 10^{-11}(L/L_{\odot})(M_{\odot}\ yr^{-1})$, derived by Scoville and Young (1983), the starbursts will consume all of the molecular gas within 6×10^7 yr in source A and within 1×10^8 yr in the summed region of sources B and C.

Noguchi and Ishibashi (1986) calculated molecular gas behavior in interacting galaxies and showed that enhanced cloud-cloud collisions induce powerful starbursts, which have similar lifetimes ($\sim 10^8$ yr) as those described above. These time scales are significantly shorter than the typical time scale ($\sim 5 \times 10^8$ yr) for the interaction of galaxies (e.g., Toomre 1977). Therefore, starbursts can be a dominant energy source only for a short time during the interaction. Arp 299 is probably in this starburst stage of the merger.

Galaxy collisions are highly inelastic. Because the change in orbital energy due to tidal interaction is always negative (Byrd, Saarinen, and Valtonen 1986), the interacting galaxies move in shrinking orbits. If large-scale tails are formed by tidal interactions, the mass in the tails carries much of the angular momentum, and a large fraction of the mass of each galaxy can sink toward their common center of mass (e.g., Schweizer 1986). Thus, much mass can be accumulated in the nucleus. In this stage, release of gravitational energy in the nucleus can be the main source of the activity. Many of the infrared ultraluminous galaxies (Sanders *et al.* 1988), which have strong evidence for active nuclei, are probably in this stage.

V. SUMMARY

Multiaperture photometric and spectroscopic observations have been obtained of the three main active regions in the interacting galactic pair Arp 299. Combining these and other observations, we reach the following conclusions:

1. There are compact red nuclei in sources A and C. The near-infrared colors of source A are similar to those of the Seyfert galaxies, while a normal galactic component with hot dust can explain the color of source C.

2. Brγ lines have been detected from sources A and C. The estimated number of ionizing photons in central 1 kpc diameter regions of sources A, B, and C are 2.7×10^{54}, 2.4×10^{54}, and 1.6×10^{54} photons s^{-1}, respectively.

3. Molecular hydrogen $v = 1 \rightarrow 0$ lines have been detected only from source A. Their ratios are consistent with shock excitation, but imply less extinction toward the H_2 emitting regions than toward H II regions.

4. Both the Brγ and the H_2 $S(1)$ lines are spatially extended, indicating that Arp 299 is undergoing an active episode of star formation on a large scale.

5. The complicated near-infrared colors and the inconsistency of the extinction derived from various observations suggest that source B consists of multiple components.

6. If the upper mass of the IMF in source A is less than 35

$M_\odot$, a simple starburst model with time evolution can explain the number of ionizing photons, the bolometric luminosities, and the luminosities of H_2 lines in each region of Arp 299, and the large L_{bol}/N_{UV} and $L_{S(1)}/L_{Br\gamma}$ ratios of source A are attributable to the rapid rate of star formation in this region. Therefore, the possible nuclear activity in source A does not dominate the luminosity and line emission.

7. The starbursts in each region of Arp 299 cannot last longer than 10^8 yr.

We are grateful to the staff of the IRTF and the UKIRT for their support and hospitality. It is a pleasure to acknowledge useful comments from Drs. M. Joy, K. Kawara, Y. Kobayashi, K. Mizutani, and the referee.

T. Nakagawa acknowledges the financial support from the Japan Society for the Promotion of Science.

REFERENCES

Allen, C. W. 1976, *Astrophysical Quantities* (London: Athlone).
Arp, H. 1966, *Atlas of Peculiar Galaxies* (Pasadena: California Institute of Technology).
Augarde, R., and Lequeux, J. 1985, *Astr. Ap.*, **147**, 273.
Beck, S. C., Turner, J. L., and Ho, P. T. P. 1986, *Ap. J.*, **309**, 70.
Black, J. H., and Dalgarno, A. 1976, *Ap. J.*, **203**, 132.
Burton, M. G., Geballe, T. R., Brand, P. W. J. L., and Webster, A. S. 1988, *M.N.R.A.S.*, **231**, 617.
Bushouse, H. A., and Gallagher, J. S., III. 1984, *Pub. A.S.P.*, **96**, 273.
Byrd, G. G., Saarinen, S., and Valtonen, M. J. 1986, *M.N.R.A.S.*, **220**, 619.
Chevalier, R. A., and Clegg, A. W. 1985, *Nature*, **317**, 44.
Condon, J. J., Condon, M. A., Gisler, G., and Puschell, J. J. 1982, *Ap. J.*, **252**, 102.
DePoy, D. L., Becklin, E. E., and Geballe, T. R. 1987, *Ap. J. (Letters)*, **316**, L63.
DePoy, D. L., Becklin, E. E., and Wynn-Williams, C. G. 1986, *Ap. J.*, **307**, 116.
Eales, S. A., Becklin, E. E., Wynn-Williams, C. G., Hodapp, K.-W., Capps, R. W., and Simons, D. A. 1987, in *Infrared Astronomy with Arrays*, ed. C. G. Wynn-Williams, E. E. Becklin, and L. H. Good (Honolulu: University of Hawaii), p. 345.
Elias, J. H., Frogel, J. A., Matthews, K., and Neugebauer, G. 1982, *A.J.*, **87**, 1029.
Fischer, J., Geballe, T. R., Smith, H. A., Simon, M., and Storey, J. W. V. 1987, *Ap. J.*, **320**, 667.
Fischer, J., Sanders, D. B., Simon, M., and Solomon, P. M. 1985, *Ap. J.*, **293**, 508.
Fischer, J., Simon, M., Benson, J., and Solomon, P. M. 1983, *Ap. J. (Letters)*, **273**, L27.
Friedman, S. D., Cohen, R. D., Jones, B., Smith, H. E., and Stein, W. A. 1987, *A.J.*, **94**, 1480.
Frogel, J. A., Persson, J. E., Aaronson, M., and Matthews, K. 1978, *Ap. J.*, **220**, 75.
Gatley, I., *et al.* 1987, *Ap. J. (Letters)*, **318**, L73.
Gehrz, R. D., Sramek, R. A., and Weedman, D. W. 1983, *Ap. J.*, **267**, 551 (GSW).
Giles, K. 1977, *M.N.R.A.S.*, **180**, 57P.
Glass, I. S. 1984, *M.N.R.A.S.*, **211**, 461.
Glass, I. S., and Moorwood, A. F. M. 1985, *M.N.R.A.S.*, **214**, 429.
Heckman, T. M., Armus, L., and Miley, G. K. 1987, *A.J.*, **92**, 276.
Hollenbach, D. J., and Shull, J. M. 1977, *Ap. J.*, **216**, 419.
Hyland, A. R., and Allen, D. A. 1982, *M.N.R.A.S.*, **199**, 943.
Joseph, R. D., Wright, G. S., Wade, R., Graham, J. R., Gatley, I., and Prestwich, A. H. 1987, in *Star Formation in Galaxies* (NASA CP-2466), ed. Carol J. Lonsdale Persson (Washington, D.C.: National Aeronautics and Space Administration), p. 247.
Joy, M., Lester, D. F., Harvey, P. M., Telesco, C. M., Decher, R., Rickard, L. J., and Bushouse, H. 1989, *Ap. J.*, **339**, 100.
Kawara, K., Nishida, M., and Gregory, B. 1987, *Ap. J. (Letters)*, **321**, L35.
Larson, R. B., and Tinsley, B. M. 1978, *Ap. J.*, **219**, 46.
Melnick, J., Terlevich, R., and Eggleton, P. P. 1985, *M.N.R.A.S.*, **216**, 255.
Noguchi, M., and Ishibashi, S. 1986, *M.N.R.A.S.*, **219**, 305.
Oliva, E., and Moorwood, A. F. M. 1986, *Astr. Ap.*, **164**, 104.
Osterbrock, D. E. 1974, *Astrophysics of Gaseous Nebulae* (San Francisco: Freeman).
Parkes, G. E., Charles, P. A., Culhane, J. L., and Ives, J. C. 1977, *M.N.R.A.S.*, **179**, 55.
Rieke, G. H., Cutri, R. M., Black, J. H., Kailey, W. F., McAlary, C. W., Lebofsky, M. J., and Elston, R. 1985, *Ap. J.*, **290**, 116.
Rothman, L. S., *et al.* 1987, *Appl. Optics*, **26**, 4058.
Sanders, D. B., and Mirabel, I. F. 1985, *Ap. J. (Letters)*, **298**, L31.
Sanders, D. B., Soifer, B. T., Elias, J. H., Madore, B. F., Matthews, K., Neugebauer, G., and Scoville, N. Z. 1988, *Ap. J.*, **325**, 74.
Sargent, A. I., Sanders, D. B., Scoville, N. Z., and Soifer, B. T. 1987, *Ap. J. (Letters)*, **312**, L35.
Savage, B. D., and Mathis, J. S. 1979, *Ann. Rev. Astr. Ap.*, **17**, 73.
Scalo, J. M. 1986, *Fund. Cosmic Phys.*, **11**, 1.
———. 1987, in *Starbursts and Galaxy Evolution*, ed. T. X. Thuan, T. Montmerle, and J. Tran Thanh Van (Paris: Editions Frontières), p. 445.
Schweizer, F. 1986, *Science*, **231**, 227.
Scoville, N., and Young, J. S. 1983, *Ap. J.*, **265**, 148.
Soifer, B. T., *et al.* 1984, *Ap. J. (Letters)*, **283**, L1.
Soifer, B. T., Houck, J. R., and Neugebauer, G. 1987, *Ann. Rev. Astr. Ap.*, **25**, 187.
Soifer, B. T., Neugebauer, G., Danielson, G. E., Lonsdale, C. J., Madore, B. F., and Persson, S. E. 1986, *Ap. J. (Letters)*, **303**, L41.
Soifer, B. T., Sanders, D. B., Madore, B. F., Neugebauer, G., Danielson, G. E., Elias, J. H., Persson, C. J., and Rice, W. L. 1987, *Ap. J.*, **320**, 238.
Taniguchi, Y., Kawara, K., Nishida, M., Tamura, S., and Nishida, M. 1988, *A.J.*, **95**, 1378.
Telesco, C. M., Decher, R., and Gatley, I. 1985, *Ap. J.*, **299**, 896.
Toomre, A. 1977, in *Evolution of Galaxies and Stellar Population*, ed. B. M. Tinsley and R. B. Larson (New Haven: Yale University Observatory), p. 401.
Toomre, A., and Toomre, J. 1972, *Ap. J.*, **178**, 623.
Traub, W. A., and Stier, M. T. 1976, *Appl. Optics*, **15**, 1976.
Ward, M., Allen, D. A., Wilson, A. S., Smith, M. G., and Wright, A. E. 1982, *M.N.R.A.S.*, **199**, 953.

T. R. GEBALLE: Joint Astronomy Centre, 665 Komohana Street, Hilo, HI 96720

HIDEO MATSUHARA, TAKAO NAKAGAWA, HARUYUKI OKUDA, and HIROSHI SHIBAI: The Institute of Space and Astronautical Science, 1-1, Yoshino-dai 3-chome, Sagamihara, Kanagawa 229, Japan

TETSUYA NAGATA: Department of Physics, Kyoto University, Kitashirakawa, Sakyou-ku, Kyoto 606, Japan